ISSN 1392 - 1207. MECHANIKA. 2008. Nr.4(72)

The rotating system vibration and diagnostics

M. Vasylius*, R. Didžiokas, P. Mažeika***, V. Barzdaitis******

**Klaipeda University, Bijūnų str. 17, 91225 Klaipėda, Lithuania, E-mail: mvasylius@yahoo.com*

***Klaipeda University, Bijūnų str. 17, 91225 Klaipėda, Lithuania, E-mail: rimantas.didziokas@ku.lt*

****Kaunas University of Technology, A. Mickevičiaus str. 37, 44244 Kaunas, Lithuania, E-mail: pranasmazeika@centras.lt*

*****Kaunas University of Technology, A. Mickevičiaus str. 37, 44244 Kaunas, Lithuania, E-mail: vytautas.barzdaitis@ktu.lt*

1. Introduction

The stationary condition monitoring, safety and diagnostic systems are mainly applied to technologically critical, expensive machines and based on vibration and technological parameters measurements [1 - 6]. The air blower machine SF01-18 is the high efficiency technological equipment operating in continuous long term running mode in the chemical plant JSC Lifosa, Fig. 1. The machine's induction electric motor EM vibration sources were identified and eliminated [2]. The motor experimental testing, modeling and simulation explained the main reason of high vibration level - insufficient dynamic stiffness of rotor with journal bearings. In this article the condition and failure diagnostics of the radial tilting-pad journal bearings of the blower rotor BR is monitored, experimentally tested modeled and results implemented in industry.

2. Air blower condition monitoring and diagnostics

The air blower machine SF01-18 comprises electric motor EM, gear box GB and blower rotor BR, as shown in Fig. 1. The 5.6 MW power induction electric motor runs at 1500 rpm and rotates an air blower rotor BR through flexible 8 pin type coupling C1, gear box GB and flexible coupling C2 at 3119 r/min.

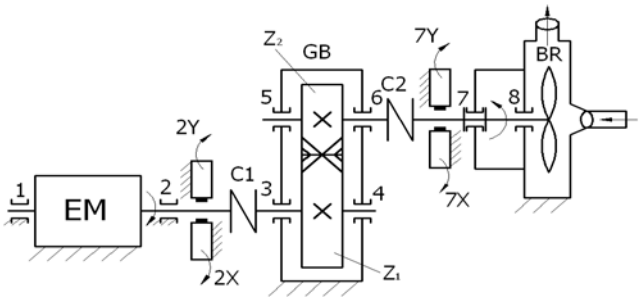

Fig. 1 The air blower and proximity probes location scheme: *1, 2* – journal bearings of EM; *3-6* – journal bearings of gearbox (GB) with transmission ratio u = 0.477 (z_2 = 43 of driven gear and z_1 = 90 of driving gear); *7, 8* – tilting-pad journal bearings of blower rotor (BR); *C1, C2* – flexible couplings; *2X, 2Y* and *7X, 7Y* – proximity probes fixed at the 2nd and 7th bearings

For experimental measurements the following test and diagnostic equipment has been used: Dynamic Machine Analyser DMA04 (Epro, Germany, Profess s.r.o., Czech Republic), portable high technology vibration signal analyzer A4300, DDS2000 Database (Adash s.r.o. Czech Republic). The technical condition is evaluated by monitoring bearings housings vibration periodically and BR rotor shaft vibration displacements permanently.

This article concerns dynamic behavior of the blower rotor BR tilting-pad journal bearings. The task is to determine the main reason of the journal bearings failure. The blower rotor shaft vibration displacement $s_{p\text{-}p7}$ and s_{max7} values at 7th bearing and maximum vibration displacement s_{max} values of the shaft at the middle location point between 7th and 8th bearings are monitored by means of 7X, 7Y proximity probes, Fig. 2. Additionally, the vibration displacement of EM 2nd bearing was monitored periodically with proximity probes 2X, 2Y and evaluates technical condition not only of 2nd bearing but flexible coupling C1 too.

The failure of 7th (Fig. 3) and 8th tilting-pad journal bearings caused additional experimental testing and theoretical modeling of blower rotor dynamics.

Fig. 2 The blower rotor vibration displacements $s_{p\text{-}p7}$, s_{max7} and shaft position measurement proximity probes location

Fig. 3 Damaged 7th tilting-pad journal bearing elements

The experimental testing of the blower rotor vibration was made at different loading: at 100% and 50% of nominal loading and at free run. The blower rotor resonance speed as natural frequency of the BR was measured during machine coast down and compared after one year

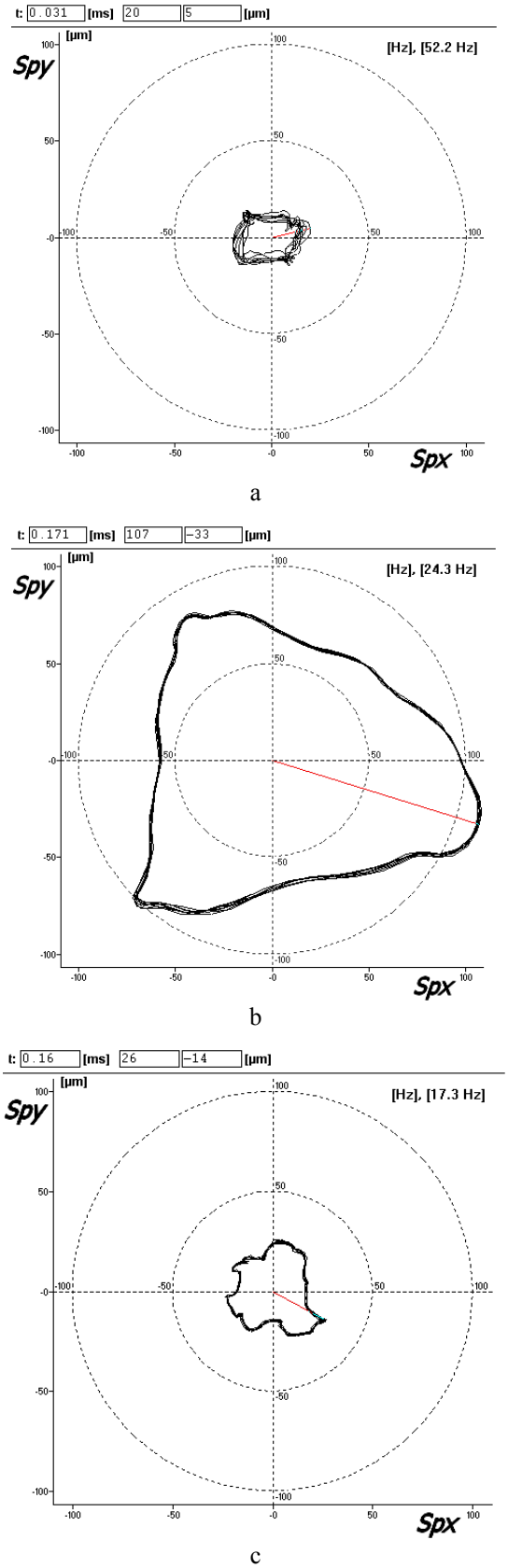

Fig. 4 The blower rotor 7th bearing shaft kinetic orbits: a) at full loading: s_{max} = 21 µm at 3132 rpm (52.2 Hz) steady-state rotational speed; b) at coast down running mode: s_{max} = 112 µm at 1458 rpm (24.3 Hz) resonance speed; c) at coast down running mode: s_{max} = 30 µm at 1038 rpm (17.3 Hz) low rotational speed

continuous operation measurement data. The BR 7th bearing shaft kinetic orbits at full loading and coast down running mode are presented in Fig. 4, a, b and c (all plots drawing scale is the same).

The peak-to-peak vibration displacement values at resonance rotational speed 1455 rpm reached inaccessible values in both X and Y orthogonal directions as shown by kinetic orbit of the shaft, Fig. 4, b. These vibration displacements $s_{p\text{-}p}$ values became 6-8 times higher at the resonance in comparison with the values at the maximum loading and nominal rotational speed 3119-3132 rpm (Fig. 4, a) and 4-5 times higher at the resonance in comparison with low rotational speed (Fig. 4, c). The maximum vibration displacement peak-to-peak value $s_{p\text{-}pmax}$ during coast down at resonance rotational speed reaches 350-420 µm. At run up mode the maximum vibration displacement peak-to-peak value $s_{p\text{-}pmax}$ at resonance reaches 200-220 µm.

The blower rotor high vibration displacements at resonance mode damage the journal bearings during coast down and run up operation modes. The valuable damages is checked at the upper segment of the 7th bearing (Fig. 3) and the lower segment of the 8th bearing. The main reason of damaged tilting-pad journal bearings is inadmissible vibration displacement value $s_{p\text{-}pmax}$ at resonance. In run up mode – the resonance phenomenon provide less vibration displacements in comparison with coast down running mode, because run up time interval from stand still mode up to 3119-3132 rpm took only 30 seconds and coast down time interval takes more than 900 seconds and dynamic forces have enough time to rise up at resonance and generate high vibration displacement amplitudes.

The dynamic forces that damages bearings depend not only on resonance phenomenon but on rotor gyroscopic effect too. The rotor shaft position in the 7th bearings is described by the gap A and gap B values. The gap value measured between tip of proximity probe and shaft surface is informative parameter that evaluates gyroscopic effect value acting on the bearings, when machine rotation speed changes from maximum till stand still.

The gap B value plot versus coast down real time (or running speed) is shown in Fig. 5. When machine runs in coast down mode, the gap B between the vertical sensor 7Y tip and shaft surface decreases. The rotors axes position in the 7th and 8th bearings changes in vertical plane. The measured gap B in vertical direction at the 7th bearing decreases about ~200 µm value (805 µm-607 µm = 198 µm, Fig. 5) reference to nominal position of the shaft inside the bearing at maximum rotation speed and maximum load.

The measured gap A in horizontal direction at the 7th bearing changes only by 2 µm value (678 µm-680 µm = = -2 µm,). But valuable gapA value changes took place at ~ 1100 rpm (691 µm-366 µm = 325 µm). The rubbing phenomenon of the rotating rotor shaft with bearing metal took part at 7th bearing upper pad (Fig. 3) and at 8th bearing lower pad. The rubbing process starts at resonance speed up to 224 rpm and when gravitation force of the blower rotor exceeds gyroscopic effect force.

The modeling and simulation of the blower rotor is provided including gyroscopic effect of the rotor. The main task of theoretical modeling is to evaluate forces acting on journal tilting-pad bearings and to simulate shaft kinetic orbit in the bearing.

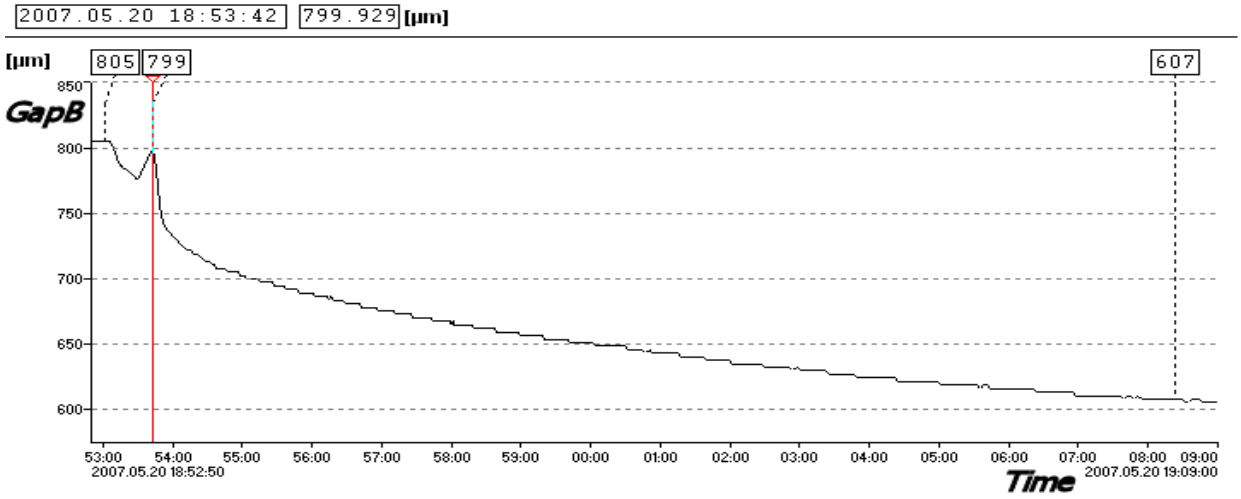

Fig. 5 The gapB values (a-vertical direction , sensor 7Y) trend plot (vertical axes–gap values in µm) versus real time (horizontal axes – time in minutes:seconds) at coast down running mode at the 7th bearing shaft: vertical direction plot - gap 805 µm at 3132 rpm, 799 µm at resonance 1450 rpm and 607 µm at 0 rpm

3. Modeling and simulation of blower rotor

The main task of theoretical modeling is to evaluate forces acting on journal tilting-pad bearings.

The second type of Lagrange equations to construct the equations of system vibration for complicated vibration system is recommended to use. These equations are applied for air blower vibration system:

$$\frac{d}{dt}\left(\frac{\partial T}{\partial \dot{q}_i}\right)-\frac{\partial T}{\partial q_i}+\frac{\partial R}{\partial \dot{q}_i}+\frac{\partial V}{\partial q_i}=F_i(t) \quad (i=1,2,...,n) \tag{1}$$

here T, V are kinetic and potential energies respectively, R is Rayleigh dissipative function, q_i are system generalized coordinates, $F_i(t)$ are external forces.

The dynamic model of all system in quiet state is showed in Fig. 6.

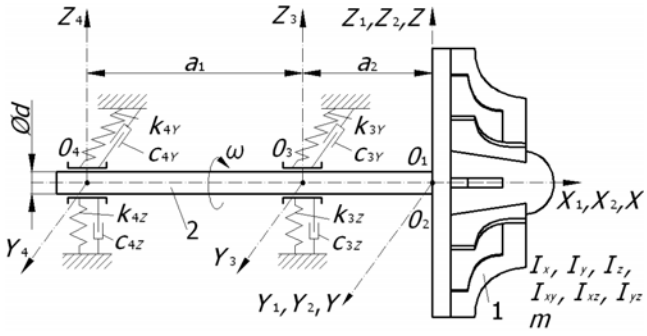

Fig. 6 Dynamic model of the air blower rotor: a_1 = 0.844 m, a_2 = 0.5m

Generalized coordinates are taken:

ξ, η are coordinates, defining position of point O_2 in the plane $O_1X_1Z_1$; φ_y, φ_z are coordinates, defining small angles about axes Y_2, Z_2.

$$q_i=\left\{\eta,\zeta,\varphi_y,\varphi_z\right\}^T \tag{2}$$

There are used three types of coordinate systems of axes to localize rotor position (Fig. 7).

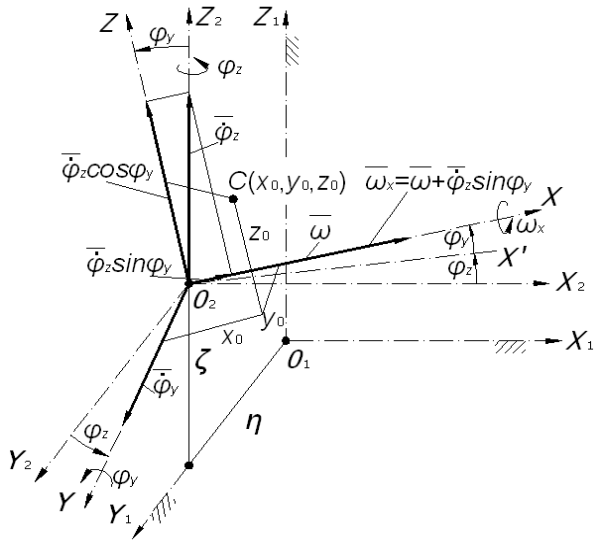

Fig. 7 The scheme of coordinates and angular velocity vectors deployment which describe the rotor position

1) Fixed coordinate system O_1 X_1 Y_1 Z_1. Point O_1 in steady state coincident with point where shaft is attached to the rotor. Weight of the rotor is not evaluated.

2) In the coordinate system O_2 X_2 Y_2 Z_2 point O_2 is tightly connected with the rotor. When the rotor rotates, center O_2 moves in plane O_1, Y_1, Z_1. Then displacement of O_2 in the system of axes $O_1X_1Y_1Z_1$ is described by generalized coordinates ζ and η.

3) System O_2XYZ tightly connected to the rotor, moving with it about point O_2. The rotor in movement can incline by small angles φ_y, φ_z about axes Y_2, Z_2 and large angle φ_x about axis X_2. Coordinates of the rotor mass center is x_0, y_0, z_0.

The kinetic energy when rotor shaft is rotating with constant angular velocity is described by Eq. (3) [7]. The influence of gyroscopic effect isn't estimated here.

$$T = \frac{1}{2}\left\{m\left(\dot{\eta}^2 + \dot{\zeta}^2\right) + I_x\omega_x{}^2 + I_y\omega_y{}^2 + I_z\omega_z{}^2\right\} -$$
$$-\left[\begin{array}{l}\left(I_{xy}cos\omega t + I_{xz}sin\omega t\right)\omega_x\omega_y + \\ \left(I_{xz}cos\omega t - I_{xy}sin\omega t\right)\omega_x\omega_z + I_{yz}\omega_z\omega_y\end{array}\right] +$$
$$+m\dot{\eta}\left[z_0\omega_x cos\omega t - x_0\omega_z - y_0\omega_x sin\omega t\right] +$$
$$+m\dot{\zeta}\left[x_0\omega_y - y_0\omega_x cos\omega t - z_0\omega_x sin\omega t\right] \qquad (3)$$

here: ω_x - shaft (not rotor) angular velocity; ω = constant; Ix, Iy, Iz, Ixy, Ixz, Iyz are moments of inertia of the rotor; m - weight of the rotor.

To estimate the influence of gyroscopic effect some new values must be included to Eq. (3). They were described in Eq. (4).

$$\begin{cases}\omega_x = \omega + \dot{\varphi}_z\, sin\varphi_y \cong \omega + \dot{\varphi}_z\varphi_y \\ \omega_y = \dot{\varphi}_y \\ \omega_z = \dot{\varphi}_z\, cos\varphi_y \cong \dot{\varphi}_z\end{cases} \qquad (4)$$

Kinetic energy equation is differentiate by generalized coordinates velocities $\dot{\eta}$, $\dot{\zeta}$, $\dot{\varphi}_y$, $\dot{\varphi}_z$ and by displacements η, ζ, φ_y, φ_z.

The received eight differential equations of motion of the rotating system are described in compact matrix form.

$$[A]\{\ddot{q}\} + [B]\{\dot{q}\} + [C]\{q\} = \{F(t)\} \qquad (5)$$

here $\{q\} = \{\xi, \eta, \varphi_y, \varphi_z\}$ is vector of generalized coordinates, $[A]$ is matrix of inertia, $[C]$ is matrix of stiffness, $[B]$ is matrix of damping and gyroscopic forces; $\{F(t)\}$ is generalized vector of external excitation, components of which are the functions of time t, angular speed ω, rotor moment of inertia.

4. Simulation results

The simulation results are shown in Fig. 8 (the plots scale is the same). They approved that vibration displacement of the rotor are caused not only by unbalance, but by gyroscopic effect too. In case of rotor center of mass shift from geometrical axis in 0.02 mm, when mass of the rotor is 2900 kg, rotational speed 3120 rpm, inertia force is 6190 N. Gyroscopic moment of the rotor have the same influence. Nominal rotational speed of the rotor is more than twice higher than its resonance frequency as experimentally measured ~23 Hz. The transient rotation running processes of BR acceleration and deceleration should be performed as fast as possible to pass resonance frequency.

Graph results corresponds the values on rotor and shat connecting point. To get the values on 3st bearing displacements Y_3 and Z_3 it is needed to multiply values of ξ and η by the coefficient, equal to 0.524, to get 4nd bearing displacement Y_4 and Z_4 it is needed multiply the mentioned values by the coefficient equal to -0.279.

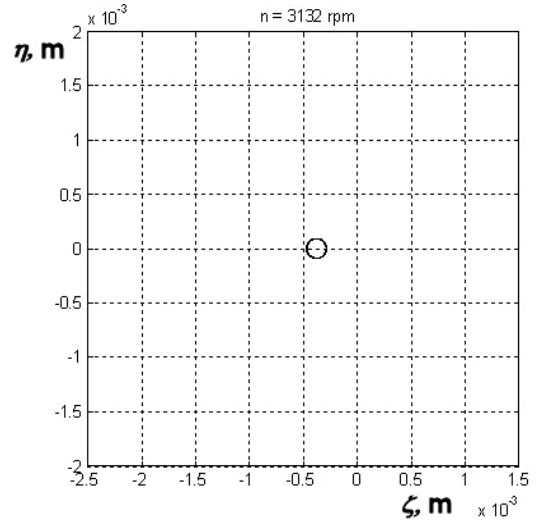

a

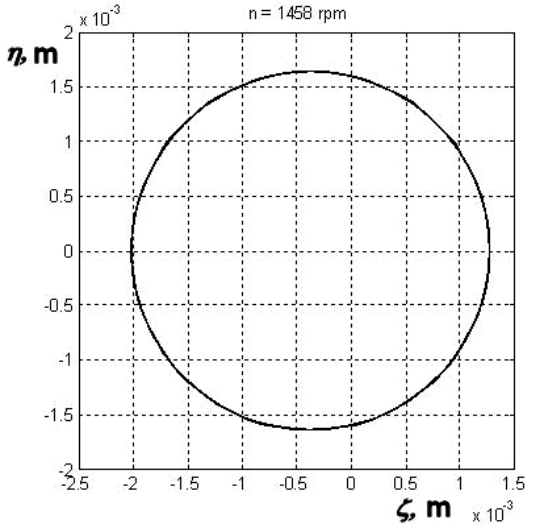

b

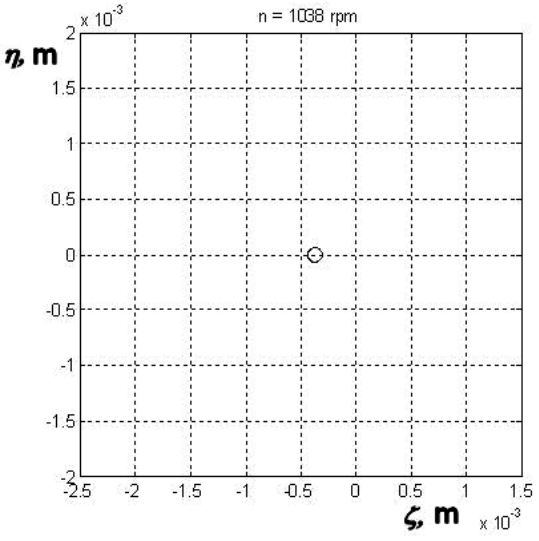

c

Fig. 8 Simulation results of the rotor with elastic supports, kinetic orbits of shaft center O_2: a) at nominal rotation speed 3132 rpm, s_{max} = 88 μm; b) at 1458 rpm resonance mode, s_{max} = 1640 μm; c) at 1038 rpm transient mode, s_{max} = 63 μm

The simulation results acquired when: mass moment of inertia of the rotor I_x = 436 kg·m^2, $I_y = I_z$ = =287 kg·m^2 and coefficients of stiffness of the support $k_{3Y} = k_{3Z} = 2 \cdot 10^8$ N/m, $k_{4Y} = k_{4Z} = 1.5 \cdot 10^8$ N/m, coefficients of damping of the support $c_{3Y} = c_{3Z}$=8000 Ns/m, $c_{4Y} = c_{4Z}$ = =4000 Ns/m.

5. Conclusions

1. The slow down mode is most dangerous running mode for the machines bearings. The shaft rubbing process starts at resonance and takes 14-15 minutes time interval till stoppage of the rotor.

2. The gyroscopic effect of the blower wheel changes shafts positions in the 7th and 8th bearings and increase rubbing process: the experiment measurements indicated that 7th baring shaft goes up (in vertical direction) ~200 μm.

3. Experimental testing results approved theoretical modeling and simulation data.

References

1. **Bently, D.E.** Fundamentals of Rotating Machinery Diagnostics. Library of Congress Control Number 2002094136, Bently Pressurized Bearing Company, printed in Canada, 2002.-726p.
2. **Barzdaitis, V., Bogdevičius, M., Gečys, St.** Vibration problems of high power air blower machine.-2nd International Symposium on Stability Control of Rotating Machinery, ISCORMA-2. Proceedings. -Gdansk, Poland; Minden, Nevada, USA, 2003, p.606-616.
3. **Barzdaitis, V., Činikas, G.** Monitoring and Diagnostics of Rotor Machines.-Kaunas: Technologija, 1998. -364p. (in Lithuanian).
4. **Goldin, A.S.** Vibration of Rotating Machines.-Moscow: Mashinostroenie, 2000.-344p. (in Russian).
5. **Vekteris, V., Čereška, A., Jurevičius, M., Striška, V.** Experimental research of rotor axis revolution orbit in rotor systems with adaptive and sleeve sliding-friction bearings. -Mechanika. -Kaunas: Technologija, 2008, Nr.2(70), p.38-42.
6. **Vasiljev A.** Simulation of valve gear dynamics using generalized dynamic model. -Mechanika. -Kaunas: Technologija, 2006, Nr.2(58), p.37-43.
7. **Bat, M.I., Dzanelidze, G.J.** Theoretical Mechanics in Examples and Problems. Vol. III. -Moscow: Nauka, 1973.-528p. (in Russian).

M. Vasylius, R. Didžiokas, P. Mažeika, V. Barzdaitis

ROTORINĖS SISTEMOS VIRPESIAI IR DIAGNOSTIKA

R e z i u m ė

Šiuolaikinių mašinų būklės stebėsenos, apsaugos ir gedimų diagnostikos sistema yra neatsiejamas netikėtų gedimų prevencijos modulis. Straipsnis skirtas chemijos pramonėje ilgalaikiu nepertraukiamu režime dirbančios orapūtės rotoriaus būklės stebėsenos, diagnostikos, modeliavimo ir gedimų prognozės tyrimams. Dinaminio modelio specifiką sudaro segmentinių slydimo guolių dinamikos įvertinimas. Orapūtės rotoriaus virpesių poslinkiai buvo matuojami bekontakčiais jutikliais, esant nominaliam apkrovimui ir įgreitinimo bei stabdymo režimams. Hipotezė apie natūralaus pobūdžio guolio gedimo efektą yra patikrinta teoriniais tyrinėjimais bei sukurtu ir imituotu dinaminiu modeliu.

M. Vasylius, R. Didžiokas, P. Mažeika, V. Barzdaitis

THE ROTATING SYSTEM VIBRATION AND DIAGNOSTICS

S u m m a r y

The condition monitoring, protection and fault diagnostics system is inherent module in the failure prevention technology of modern machines. The paper is dedicated to research of dynamics, condition monitoring,, fault diagnosis and modeling of high speed blower rotor failure prognosis. The specificity of the dynamic model comprises dynamics of the tilting-pad journal bearings. The blower rotor vibration displacements were monitored with contact less sensors during nominal load, run up and shout down modes. Hypotheses about physical nature of bearings failure effect are verified by experimental and theoretical research, where dynamical model was designed and simulated.

М. Василюс, Р. Диджекас, П. Мажейка, В. Барздаитис

ВИБРАЦИИ И ДИАГНОСТИКА РОТОРНОЙ СИСТЕМЫ

Р е з ю м е

Система мониторинга технического состояния и диагностики отказов является неотделимым модулем в технологии предотвращения отказов в современных машинах. Статья посвящена исследованию технического состояния, моделированию динамики и прогнозированию случайных отказов воздуходувки, работающей в химической промышленности в продолжительном непрерывном режиме. Специфика динамической модели состоит в оценке динамики сегментных подшипников скольжения. Вибрации вала ротора в подшипнике измерены сенсорами индукционного типа при номинальной нагрузке и в режимах ускорения и торможения машины. Гипотеза о причинах повреждения подшипника скольжения проверена теоретическими и экспериментальными исследованиями.

This research was supported by the Lithuanian State Science and Studies Foundation, Grant Nr. 51/08

Received May 06, 2008